Published in final edited form as:
Cancer Discov. 2014 July ; 4(7): 773–780. doi:10.1158/2159-8290.CD-14-0049.

Autophagy Inhibition Improves Chemosensitivity in BRAF^{V600E} Brain Tumors

Jean M. Mulcahy Levy[1], **Joshua C. Thompson**[1], **Andrea M. Griesinger**[1], **Vladimir Amani**[1], **Andrew M. Donson**[1], **Diane K. Birks**[2], **Michael J. Morgan**[3], **David M. Mirsky**[4], **Michael H. Handler**[2], **Nicholas K. Foreman**[1], and **Andrew Thorburn**[3]

[1]Department of Pediatrics, University of Colorado Denver, Aurora, CO

[2]Department of Neurosurgery, University of Colorado Denver, Aurora, CO

[3]Department of Pharmacology, University of Colorado Denver, Aurora, CO

[4]Department of Radiology, University of Colorado Denver, Aurora, CO

Abstract

Autophagy inhibition is a potential therapeutic strategy in cancer, but it is unknown which tumors will benefit. The BRAF^{V600E} mutation has been identified as important in pediatric CNS tumors and is known to affect autophagy in other tumor types. We evaluated CNS tumor cells with BRAF^{V600E} and found that mutant cells (but not wild type) display high rates of induced autophagy, are sensitive to pharmacologic and genetic autophagy inhibition, and display synergy when the clinically used autophagy inhibitor chloroquine was combined with the Raf inhibitor vemurafenib or standard chemotherapeutics. Importantly we also demonstrate chloroquine can improve vemurafenib sensitivity in a resistant *ex vivo* primary culture and provide the first demonstration in a patient harboring the V600E mutation treated with vemurafenib that addition of chloroquine can improve clinical outcomes. These findings suggest CNS tumors with BRAF^{V600E} are autophagy-dependent and should be targeted with autophagy inhibition in combination with other therapeutic strategies.

Keywords

Brain tumors; pediatric; autophagy; BRAF; chloroquine

Introduction

Despite treatment advancements in childhood central nervous system (CNS) tumors and increased long-term survival over the past 50 years, CNS tumors remain a leading cause of childhood cancer death. New treatment strategies are urgently needed. Two potential strategies are 1) targeting specific mutations with small molecule inhibitors and 2) using a broader approach by inhibiting tumor cell survival pathways such as autophagy.

Corresponding author: Jean M. Mulcahy Levy, UCDenver at Anschutz Medical Campus, Pediatrics Department, Mail Stop 8302, 12800 E. 19th Ave. Aurora, CO 80045, Tel: (303)-724-3372, Fax: (303) 724-3363, Jean.Mulcahy-Levy@childrenscolorado.org.

Conflicts of Interest: None

One of the most common mutations that can be targeted therapeutically is the V600E mutation in the v-RAF murine sarcoma viral oncogene homolog B1 (BRAF)(1), which constitutively activates BRAF, resulting in increased tumorigenic growth. Recent studies have confirmed this mutation in pediatric brain tumors (2–6) highlighting its potential as a therapeutic target for these tumors using drugs such as vemurafenib, an ATP-competitive inhibitor, which has shown success in the treatment of late-stage melanoma (7). Case reports of patients with V600E mutations in other cancers including lung adenocarcinomas (8), refractory hairy-cell leukemia (9), and multiple myeloma (10) have indicated potential therapeutic benefits of this drug. Nicolaides et al. reported the effectiveness of targeting $BRAF^{V600E}$ in the context of malignant astrocytoma (2). Furthermore, our group reported the first pediatric patient treated with vemurafenib and demonstrated the potential for clinical improvement in pediatric patients using this targeted approach (11).

Recent studies have investigated the role of autophagy in cells with BRAF mutations. The ERK pathway induces autophagy and melanoma cells with oncogenic BRAF and hyper-activation of ERK show higher levels of autophagy (12). In $BRAF^{V600E}$-driven lung tumors, autophagy was essential for mitochondrial metabolism and tumor growth, and mice where autophagy was blocked by knockout of an essential autophagy gene had a median survival nearly twice that of controls (13). Recent studies suggest that a high “autophagic index” in melanoma patient tumor biopsies is linked to poor therapeutic response and shorter survival. Furthermore, melanoma cells with high rates of autophagy had increased sensitivity and cell death with inhibition of autophagy and temozolomide compared to temozolomide alone (14).

Clinical trials evaluating the potential of autophagy inhibition in a variety of therapeutic protocols are ongoing in adult patients including those with CNS tumors (15). We hypothesized that $BRAF^{V600E}$ cells would show higher levels of autophagy and as a result, tumor cell death would increase when autophagy inhibition was combined with targeted $BRAF^{V600E}$ inhibition. We report here that high levels of autophagy are induced in $BRAF^{V600E}$ CNS tumor cells and these cells, but not BRAF wild-type (WT) cells, are highly sensitive to genetic and pharmacologic inhibition of autophagy. Moreover, inhibition with clinically available drugs is synergistic with both small molecule inhibition of $BRAF^{V600E}$ and other chemotherapeutics in these tumors. And we demonstrate that chloroquine can improve clinical efficacy of vemurafenib in a patient with a $BRAF^{V600E}$ tumor.

Results

During autophagy, LC3 is cleaved then conjugated to phosphatidylethanolamine to create LC3-II and incorporated into the autophagosomal membrane. Autophagy can be measured by monitoring LC3-II on western blots, by microscopy, or by flow cytometry using fluorescent protein-tagged LC3(16). Using a tandem mCherry (mCh)-GFP-LC3 expression construct, changes in autophagy can be more quantitatively monitored in a cell population by measuring the ratio of GFP to mCh by flow cytometry. Employing this method, we evaluated multiple $BRAF^{V600E}$ mutant cell lines for autophagy induction in response to amino acid starvation, the current gold standard. Three astrocytoma cell lines, NMC-G1,

DBTRG, and AM38, have previously characterized $BRAF^{V600E}$ mutations, with AM38 showing homozygosity and the remainder heterozygosity (2). The 794 cell line was established and characterized in our lab from a ganglioglioma that developed a secondary atypical tertaoid/rhabdoid tumor (ATRT) component. The 794 cells exhibit both INI-1 loss and the presence of $BRAF^{V600E}$ (5). This line provides an ideal *in vitro* model to test the effectiveness and specificity of vemurafenib in the context of a pediatric brain tumor, as it allows for stable, long-term growth that is otherwise difficult to achieve with low-grade tumors. V600E mutations in ATRTs evolved from a ganglioglioma or pleomorphic xanthoastrocytoma (PXA) have been previously noted (4).

Under starvation stress (Fig. 1A), all $BRAF^{V600E}$ cells induced autophagy to a greater degree than WT cells. This was confirmed by imaging of starved GFP-LC3 cells with and without chloroquine (CQ). Chloroquine prevents lysosomal fusion with autophagosomes resulting in the build up of membrane-bound LC3 that allows the quantification of GFP puncta pre- and post-CQ. Increased autophagic flux was demonstrated by an increased number of GFP puncta in starved cells with CQ compared to starvation alone (Supplemental Fig. 1A). $BRAF^{V600E}$ cells showed a higher median number of puncta per cell compared to WT (Supplemental Fig. 1B).

To establish whether autophagy inhibition would be an effective therapeutic intervention in $BRAF^{V600E}$ cells, we measured cell survival after pharmacologic or genetic autophagy inhibition. $BRAF^{V600E}$ cells expressing shRNAs targeting Atg5 or Atg12 showed a 50% or greater reduction in the number of metabolically active cells compared to their non-target (NT) controls by MTS assay (Fig. 1B). This corresponded to an increase in propidium iodide positive (PI+) 794 and AM38 cells (Supplemental Fig. 2A). In comparison, BT16 $BRAF^{WT}$ cells displayed only a minimal survival defect with Atg5 knockdown and no change with Atg12 knockdown (Fig. 1B) with a similar lack of PI+ cells (Supplemental Fig 2A). Visualizing growth of $BRAF^{V600E}$ cells with continuous microscopic imaging demonstrated substantial decreased growth velocity of the knockdown cells compared to NT controls. The growth velocity of the BT16 $BRAF^{WT}$ cells was slightly affected, but the effect was much stronger in the $BRAF^{V600E}$ cells (Fig. 1C). Cells were verified to have effective RNAi of autophagy related proteins (Fig. 1D) and a resultant high degree of autophagy inhibition (Supplemental Fig. 2B).

Because CQ is a potent autophagy inhibitor, which is FDA-approved and available for rapid translation to pediatric clinical trials, we evaluated its effects on our CNS tumor cells. $BRAF^{V600E}$ positive and WT BT16 cells were treated with increasing doses of CQ and cell death/viability was assessed by lactate dehydrogenase (LDH) release and MTS assay (Fig. 1E). $BRAF^{V600E}$ cells showed significantly higher LDH release than WT cells and a much greater loss of cell viability by MTS assay. Importantly, these effects were not seen in WT RAF cells suggesting the BRAF mutation makes the survival of brain cancer cells autophagy-dependent even under non-stressed conditions. $BRAF^{V600E}$ positive cells also demonstrated a higher percentage of PI+ cells with CQ compared to $BRAF^{WT}$ cells (Fig. 1F). The number of PI+ cells correlated with growth of the cells exposed to CQ. AM38, 794, and NMC-G1 cells demonstrated negative or flat growth rates at doses higher than 12.5 μM (Supplemental Fig. 3A), also consistent with the dose ranges at which the cells released

LDH. This also correlated to onset of strong autophagy inhibition demonstrated by LC3II accumulation in all lines by a dose of 25 μM CQ (Supplemental Fig. 3B).

Our previous studies in pediatric CNS cell lines with no RAF mutations found little difference in chemosensitivity when autophagy was inhibited (17). In contrast, the pharmacologic inhibition of autophagy improved the effectiveness of vemurafenib in combination with CQ in $BRAF^{V600E}$ 794 and AM38 cells. When $BRAF^{WT}$ cells are treated with a similar range of doses of vemurafenib there was a minimal effect on cell viability with the addition of CQ (Fig. 2A). Treating with a 100 times higher dose to produce a true dose curve also failed to show a significant improvement in the effectiveness of vemurafenib in combination with CQ in the $BRAF^{WT}$ cells (Supplemental Fig. 4). When treated with a broader range of doses of both drugs, the resultant Chou-Talalay combination indices (CI) were all less than 1 in the $BRAF^{V600E}$ cells, indicating synergy at all doses tested (Fig 2B). The most profound synergy occurred in the low nM vemurafenib doses with 5–10 μM CQ. Importantly, these doses are in the clinically achievable range for CQ (18). Conversely in the $BRAF^{WT}$ cells, at clinically relevant vemurafenib doses the addition of CQ was predominantly antagonistic (Fig. 2B). Vemurafenib treatment had little effect on autophagic flux in any of the cells (Supplemental Fig. 5) suggesting that synergy with autophagy inhibition is not a consequence of the drug itself inducing autophagy but rather a reflection of the combined effects of targeting two essential components in BRAF mutant cells– i.e. autophagy and Raf signaling.

To investigate if synergy in $BRAF^{V600E}$ cells also applied to other drugs, we evaluated combination therapy with cisplatin and vinblastine (Fig. 2C and 2E). CQ increased tumor cell death in 794 and AM38 with both drugs, but not in the WT BT16 cells. Evaluation of the synergistic potential of these combinations (Fig. 2D and 2F) found that in 794 cells, cisplatin CI values less than 1 were obtained for doses less than 12.5 μM with CQ doses as low as 5 μM and improving as the CQ dose increased in most cases. This was true for AM38 as well though at 40 μM CQ the majority of the evaluated cells were dead at all doses of cisplatin. Similar findings were seen for vinblastine with synergy seen at low doses of cisplatin and CQ doses starting at 5 μM and generally improving with increasing concentration. WT BT16 cells again demonstrated an antagonistic effect of combination therapy with both cisplatin and vinblastine with CI values predominantly above 1.

To ensure these findings were germane to true low-grade tumors with the mutation, we tested $BRAF^{V600E}$-positive primary PXA samples. We evaluated two cell lines derived from $BRAF^{V600E}$-positive PXA (Fig. 3A). UPN 858-2 and 794 lines had similar responses and IC50 to vemurafenib (111 nM and 273 nM, respectively). In contrast, UPN678 displayed signs of resistance with an IC50 of 11 μM (Fig. 3A). We therefore evaluated whether the relatively vemurafenib-resistant UPN678 cell line could be sensitized with CQ (Fig. 3B). Combination therapy produced additive effects at 5–10 μM CQ starting at 300 nM vemurafenib. With the addition of 10 uM CQ, the IC50 for these cells decreased to 4.2 μM, suggesting that CQ can overcome vemurafenib resistance.

Our group previously reported the case of a patient with a recurrent $BRAF^{V600E}$ mutant brainstem ganglioglioma successfully treated with vemurafenib and vinblastine (11). This

patient continued to do well with this regimen for approximately one year until she presented with re-onset of progressive hiccups lasting up to 23 hours per day and a new left facial weakness (Fig. 4A). MR imaging found increased FLAIR hyperintensity at the pontomedullary junction, the site of her previous recurrence, and a slight increase in the overall size of her medullary mass (Fig. 4B) suggesting acquired vemurafenib resistance as is commonly seen in melanoma patients (19). Vinblastine was stopped and due to prior radiation injury she was not a candidate for re-irradiation. After discussion with the family she continued on vemurafenib with the addition of CQ in an attempt to improve vemurafenib's therapeutic effect. Use of CQ in adult CNS tumor patients had been previously published (20, 21) and this patient was treated similarly with 150mg/d of CQ while continuing on standard dose vemurafenib. She showed rapid clinical improvement and within six weeks had a 90% reduction in hiccup duration with significant improvement in her left facial nerve palsy. On imaging, there was significant improvement in the FLAIR signal abnormality in the pontomedullary junction and resolution of the abnormality by 4 months. Six months into therapy, there was continued clinical improvement, resolution of FLAIR signal abnormality, and stabilization of her medullary mass with no further tumor growth (Fig. 4C).

With continued monitoring, the patient had periods of time requiring discontinuing vemurafenib, resulting in single drug therapy with CQ alone. During these time periods she showed clinical and MRI evidence of disease advancement that resolved with the reinitiation of vemurafenib treatment. Therefore in this patient, neither the vemurafenib and vinblastine combination therapy nor the CQ alone was effective once resistance developed, but the vemurafenib and CQ in combination were able to stabilize her disease for, currently, more than 16 months. This suggests that the clinical improvement fits with the mechanism we found in cell culture–$BRAF^{V600E}$-driven autophagy making cells sensitive to autophagy inhibition to increase the efficacy of the RAF inhibitor– rather than being a response to the CQ alone. A comprehensive outline of her clinical course is shown in Supplementary Fig 6.

Discussion

There are over three-dozen active clinical trials in adult cancer patients exploring autophagy inhibition (15, 22) and similar trials in pediatric patients are likely to be forthcoming. These trials should target patients who will most likely benefit from this intervention by determining the tumor types and genetic lesions that increase sensitivity to autophagy inhibition. The link between of autophagy and $BRAF^{V600E}$ is becoming clear as shown by its importance in the growth of lung tumors harboring the mutation (13). Our data suggest a similar important role for autophagy in pediatric CNS tumors with BRAF mutation and, importantly, show that similar tumors without this mutation do not display a robust response to autophagy inhibition or synergy with other drugs when autophagy is inhibited. A recent paper reported that targeting ER stress induced autophagy can overcome $BRAF^{V600E}$ inhibitor resistance in melanoma suggesting these effects may occur in other tumor types as well (23).

There is expanding interest in the use of targeting therapy against the V600E mutation in the pediatric brain tumor population. More patients will continue to be treated with RAF-

inhibitors, particularly as results become available from ongoing clinical trials such as the first trial in pediatric brain tumor patients, the Phase 0 and Pilot Efficacy Study in Children with Recurrent or Refractory $BRAF^{V600E}$-mutant Gliomas (24). Our group reported on the first patient treated with vemurafenib (11) and since that time an additional three patients have been reported (25). One of these patients died of an intracranial hemorrhage following two weeks of, but of the remaining two patients, one demonstrated a durable clinical response at 20 months while the other had progressive disease following two months of therapy. With the additional experience of our patient showing progressive disease following 11 months of therapy with vemurafenib, it is clear that CNS tumor patients acquire resistance to vemurafenib and rational combination therapies are needed to improve the overall potential for RAF-inhibitors.

The clinical response reported here is the first case where a deliberate attempt at autophagy inhibition improved the response to another drug in a person with recurrent disease showing signs of acquired resistance and suggests that, as in the *in vitro* experiments, CQ treatment led to an improved vemurafenib response. These data highlight an exciting possibility for identifying genetic markers, such as $BRAF^{V600E}$, which sensitize tumors to autophagy inhibition combination therapy. Importantly, with this particular genetic marker, synergy was identified with both a specific, targeted therapy and other chemotherapies as well, suggesting that synergistic interactions are governed by the autophagy-dependence of the tumor driven by its underlying mutations rather than being specific to the combined drugs. Therefore, in autophagy-dependent tumors such as those with $BRAF^{V600E}$ there may be broad potential application of autophagy inhibition.

Materials and Methods

Study Approval

Primary patient samples were obtained from Children's Hospital Colorado and collected in accordance with local and Federal human research protection guidelines and institutional review board regulations (COMIRB 95–500). Informed consent was obtained for all specimens collected.

Statistics

Statistical comparisons were completed using one-way ANOVA 9 (GraphPad Prism 5.0). A P-value of less than 0.05 was considered statistically significant. Data shown are mean ± SD except where indicated.

Reagents and cell lines

Vemurafenib was obtained from LC Laboratories (Woburn, MA). BT16 ATRT cells were kindly provided as a gift from Dr. Peter Houghton (St. Jude Children's Research Hospital, Memphis, TN). U87 and DBTRG-05 cell lines were purchased from American Type Cell Culture (Rockville, MD). AM38 and NMC-G1 cell lines were purchased from the Japan Health Sciences Foundation Health Science Research Resources Bank (Osaka, Japan). 794 cells were established from a sample obtained during routine surgery at diagnosis. Cell lines were maintained in media supplemented with 10% fetal bovine serum (FBS) (Gibco,

Carlsbad, CA) at 37°C in a humidified chamber of 5 % CO2. The 794 line required Opti-MEM (Gibco) supplemented with 15% FBS. Cell line authentication was performed using short tandem repeat profiling and comparison to known cell line DNA profiles.

LDH Assay

Cells were seeded at 2,000–4,000 cells per well, dependent on optimal conditions per line, in 96-well plates (Corning, Corning, NY) and incubated overnight. Cells were treated with increasing doses of CQ (Sigma, St. Louis, MO) for 48 hours. LDH release was quantitated using the Cytoscan-LDH Cytotoxicity Assay Kit (G-Biosciences, St. Louis, MO) according to manufacturer's instructions.

MTS Assay

Cells were seeded at 2,00 to 4,000 cells, dependent on optimal conditions per line, in 96-well plates (Corning, Corning, NY). RNAi cells were plated 48 hours after knockdown. Cells were treated as indicated for 48 to 72 hours dependent on experimental conditions. Viable cells were measured using the 3-(4,5-dimethylthiazol-2-yl)-5-(3-carboxymethoxyphenyl)-2-(4-sulfophenyl)-2H-tetrazolium salt (MTS) assay with CellTiter 96 AQueous One Solution Reagent (Promega, Madison, WI) following the manufacturer's protocol. The optical density of each well was measured with a Biotek Synergy 2 microplate reader (Winooski, VT) at 490 nm. The proportion of cells per treatment group was normalized to control wells.

Tritiated Thymidine Uptake

Cell proliferation was determined by 3H-thymidine incorporation. Cells were seeded and treated with drug as indicated. Mitomycin C (25 mg/mL) was included as a negative control. Cells were pulsed with 0.5 mCi 3H-thymidine and incubated at 37°C for 4 hours prior to cell harvest. After pulsing, short-term cultures were incubated overnight due to their slower rate of growth. Wells were washed with PBS and 6% trichloroacetic acid was added to each well for 1 hr at 4°C. Wells were washed with 1mL cold 6% trichloroacetic acid and the acid precipitate was dissolved overnight in 50 μL 0.5N NaOH. This solution was transferred to scintillation vials containing 3ml of ScintiSafe-30% and incorporated radioactivity was measured using a scintillation counter. DMSO showed no effect in control assays performed.

Combination index synergy measurement

The combination index was calculated by the Chou-Talalay equation, which takes into account both the potency (IC50) and shape of the dose-effect curve (the M-value)(26). Combination index values less than 1, equal to 1, and more than 1 indicate synergism, additive effect, and antagonism, respectively.

shRNA Transfection

A pLKO system (Sigma-Aldrich, St. Louis, MO) was utilized for RNAi of autophagy related proteins. TRC numbers for shRNAs used are: ATG5 (#151474), ATG12 (#7392), non-target (SHC016). Cells were transduced with lentivirus using 8ug/mL polybrene and

selected with the puromycin dose determined appropriate for each cell line. Level of targeted knockdown was determined by western blot.

Western Immunoblots

Cell lysates were harvested after treatments and timepoints indicated using RIPA buffer (Sigma, St. Louis, MO) with phosphatase inhibitors (Roche, Indianapolis, IN). Membranes were blocked in PBS-Tween 5% milk and probed with primary antibodies at manufacturer recommended concentrations. Anti-β-actin (Sigma, St. Louis, MO) was used as the protein loading control. Primary antibodies used were: ATG5, ATG12 and LC3 (Novus Biologicals, Littleton, CO).

Flow Cytometry

Cells constitutively expressing mCherry-GFP-LC3 were seeded at 2×10^5 in 60 mm plates and allowed to equilibrate overnight. Cells were exposed to either standard media, Earl's Based Salt Solution (EBSS) starvation media (Sigma, St. Louis, MO) or vemurafenib as indicated for evaluation of induced autophagy. Flow data was acquired on a Gallios561 and analyzed using Summit v5.1 (Beckman Coulter, Fort Collins, CO). Autophagic flux was determined by the ratio of mCherry:GFP.

IncuCyte Growth Monitoring

Cells were seeded at 2,000 cells per well in a 96-well plate (Costar, Corning, NY). Cells were cultured at 37° and 5% CO_2 and monitored using an Incucyte Zoom (Essen BioScience, Ann Arbor, MI). Images were captured at 4-hour intervals from 4 separate regions per well using a 10× objective. Each experiment was done in triplicate and growth curves were created from confluence measurements.

MRI Images

MRI images were obtained using standard protocols on a Siemens 1.5T Avanto (Munich, Germany) scanner.

Propidium Iodide Staining

Cells were seeded at 1×10^5 cells per well on a 6-well plate (Corning). RNAi cells were plated 48 hours after knockdown and analyzed after 72 hours of additional growth. CQ treated cells were harvested 48 hours post-treatment. The percentage of PI positive cells was determined using the Vybrant Apoptosis Assay Kit #4 according to the manufacturer's protocol. (Life Technologies, Grand Island, NY). Flow data was acquired on a Gallios561 and analyzed using FloJo version 10.07 (Treestar, Ashland, OR). Data was normalized to control wells.

Microscopy

Cells constitutively expressing mCherry-GFP-LC3 were seeded onto poly-D-lysine coated cell culture slides (BD Biosciences, San Jose, CA) and treated for four hours in media with or without 10 μM CQ and EBSS (Sigma, St. Louis, MO) with or without 10 μM CQ. Cells were fixed with 4% paraformaldehyde and imaged at 100× on a 3i Marianas Spinning Disk

Confocal Microscope. Imaging was performed in the University of Colorado Anschutz Medical Campus Advance Light Microscopy Core. Quantification of GFP-LC3 puncta was done using the ITCN nuclei counter on ImageJ 1.48a.

Supplementary Material

Refer to Web version on PubMed Central for supplementary material.

Acknowledgments

This work was supported by an elope, Inc. St. Baldrick's Foundation Scholar Award, NIH/NICHD Child Health Research Career Development Award (K12 HD068372) and Hyundai Hope on Wheels (JML). The Morgan Adams Foundation (NF); NIH/NCI R01CA150925 and CA111421 (AT). NIH/NCRR Colorado CTSI Grant Number UL1 RR025780 (Microscopy core). Shared resources Cancer Center Support Grant (P30CA046934) (Flow Cytometry Core).

Abbreviations

CQ	chloroquine
CNS	central nervous system
CI	combination indices
FBS	fetal bovine serum
LDH	lactate dehydrogenase
mCh	mCherry
NT	non-target
PXA	pleomorphic xanthoastrocytoma
PI	propidium iodide
WT	wild type
BRAF	v-RAF murine sarcoma viral oncogene homolog B1

References

1. Davies H, Bignell GR, Cox C, Stephens P, Edkins S, Clegg S, et al. Mutations of the BRAF gene in human cancer. Nature. 2002; 417:949–954. [PubMed: 12068308]
2. Nicolaides TP, Li H, Solomon DA, Hariono S, Hashizume R, Barkovich K, et al. Targeted therapy for BRAFV600E malignant astrocytoma. Clin Cancer Res. 2011; 17:7595–7604. [PubMed: 22038996]
3. Dias-Santagata D, Lam Q, Vernovsky K, Vena N, Lennerz JK, Borger DR, et al. BRAF V600E mutations are common in pleomorphic xanthoastrocytoma: diagnostic and therapeutic implications. PLoS One. 2011; 6:e17948. [PubMed: 21479234]
4. Dougherty MJ, Santi M, Brose MS, Ma C, Resnick AC, Sievert AJ, et al. Activating mutations in BRAF characterize a spectrum of pediatric low-grade gliomas. Neuro Oncol. 2010; 12:621–630. [PubMed: 20156809]
5. Kleinschmidt-DeMasters BK, Birks DK, Aisner DL, Hankinson TC, Rosenblum MK. Atypical teratoid/rhabdoid tumor arising in a ganglioglioma: genetic characterization. The American journal of surgical pathology. 2011; 35:1894–1901. [PubMed: 22082607]

6. Schindler G, Capper D, Meyer J, Janzarik W, Omran H, Herold-Mende C, et al. Analysis of BRAF V600E mutation in 1,320 nervous system tumors reveals high mutation frequencies in pleomorphic xanthoastrocytoma, ganglioglioma and extra-cerebellar pilocytic astrocytoma. Acta Neuropathol. 2011; 121:397–405. [PubMed: 21274720]
7. Chapman PB, Hauschild A, Robert C, Haanen JB, Ascierto P, Larkin J, et al. Improved survival with vemurafenib in melanoma with BRAF V600E mutation. N Engl J Med. 2011; 364:2507–2516. [PubMed: 21639808]
8. Gautschi O, Pauli C, Strobel K, Hirschmann A, Printzen G, Aebi S, et al. A patient with BRAF V600E lung adenocarcinoma responding to vemurafenib. J Thorac Oncol. 2012; 7:e23–e24. [PubMed: 22743296]
9. Dietrich S, Glimm H, Andrulis M, von Kalle C, Ho AD, Zenz T. BRAF inhibition in refractory hairy-cell leukemia. N Engl J Med. 2012; 366:2038–2040. [PubMed: 22621641]
10. O'Donnell E, Raje NS. Targeting BRAF in Multiple Myeloma. Cancer discovery. 2013; 3:840–842. [PubMed: 23928771]
11. Rush S, Foreman N, Liu A. Brainstem ganglioglioma successfully treated with vemurafenib. J Clin Oncol. 2013; 31:e159–e160. [PubMed: 23358987]
12. Maddodi N, Huang W, Havighurst T, Kim K, Longley BJ, Setaluri V. Induction of autophagy and inhibition of melanoma growth in vitro and in vivo by hyperactivation of oncogenic BRAF. J Invest Dermatol. 2010; 130:1657–1667. [PubMed: 20182446]
13. Strohecker AM, Guo JY, Karsli-Uzunbas G, Price SM, Chen GJ, Mathew R, et al. Autophagy sustains mitochondrial glutamine metabolism and growth of BrafV600E-driven lung tumors. Cancer discovery. 2013; 3:1272–1285. [PubMed: 23965987]
14. Ma XH, Piao S, Wang D, McAfee QW, Nathanson KL, Lum JJ, et al. Measurements of tumor cell autophagy predict invasiveness, resistance to chemotherapy, and survival in melanoma. Clin Cancer Res. 2011; 17:3478–3489. [PubMed: 21325076]
15. Levy JM, Thorburn A. Targeting autophagy during cancer therapy to improve clinical outcomes. Pharmacol Ther. 2011; 131:130–141. [PubMed: 21440002]
16. Klionsky DJ, Abdalla FC, Abeliovich H, Abraham RT, Acevedo-Arozena A, Adeli K, et al. Guidelines for the use and interpretation of assays for monitoring autophagy. Autophagy. 2012; 8:445–544. [PubMed: 22966490]
17. Levy JM, Thorburn A. Modulation of pediatric brain tumor autophagy and chemosensitivity. J Neurooncol. 2012; 106:281–290. [PubMed: 21842312]
18. Augustijns P, Geusens P, Verbeke N. Chloroquine levels in blood during chronic treatment of patients with rheumatoid arthritis. European journal of clinical pharmacology. 1992; 42:429–433. [PubMed: 1307690]
19. Trunzer K, Pavlick AC, Schuchter L, Gonzalez R, McArthur GA, Hutson TE, et al. Pharmacodynamic effects and mechanisms of resistance to vemurafenib in patients with metastatic melanoma. J Clin Oncol. 2013; 31:1767–1774. [PubMed: 23569304]
20. Briceno E, Calderon A, Sotelo J. Institutional experience with chloroquine as an adjuvant to the therapy for glioblastoma multiforme. Surgical neurology. 2007; 67:388–391. [PubMed: 17350410]
21. Sotelo J, Briceno E, Lopez-Gonzalez MA. Adding chloroquine to conventional treatment for glioblastoma multiforme: a randomized, double-blind, placebo-controlled trial. Ann Intern Med. 2006; 144:337–343. [PubMed: 16520474]
22. Amaravadi RK, Lippincott-Schwartz J, Yin XM, Weiss WA, Takebe N, Timmer W, et al. Principles and Current Strategies for Targeting Autophagy for Cancer Treatment. Clin Cancer Res. 2011; 17:654–666. [PubMed: 21325294]
23. Ma XH, Piao SF, Dey S, McAfee Q, Karakousis G, Villanueva J, et al. Targeting ER stress-induced autophagy overcomes BRAF inhibitor resistance in melanoma. J Clin Invest. 2014; 124:1406–1417. [PubMed: 24569374]
24. Safety and Phase 0 Study of vemurafenib, and oral inhibitor of BRAFV600E in Children with Recurrent/Refractory BRAFV600E-mutant gliomas. Pacific Pediatric Neuro-Oncology Consortium. [Internet] Available from: http://www.pnoc.us/clinical-trials/safety-and-phase-0-study-vemurafenib-oral-inhibitor-brafv600e-children.

25. Bautista F, Paci A, Minard-Colin V, Dufour C, Grill J, Lacroix L, et al. Vemurafenib in pediatric patients with BRAFV600E mutated high-grade gliomas. Pediatr Blood Cancer. 2014; 61:1101–1103. [PubMed: 24375920]

26. Chou TC, Talalay P. Quantitative analysis of dose-effect relationships: the combined effects of multiple drugs or enzyme inhibitors. Advances in enzyme regulation. 1984; 22:27–55. [PubMed: 6382953]

Statement of Significance

Autophagy inhibition may improve cancer therapy but it is unclear which tumors will benefit. We found that BRAF mutations cause brain tumor cells to depend on autophagy and display selective chemosensitization with autophagy inhibition. We present a pediatric case where deliberate autophagy inhibition halted tumor growth and overcome acquired BRAF-inhibition resistance.

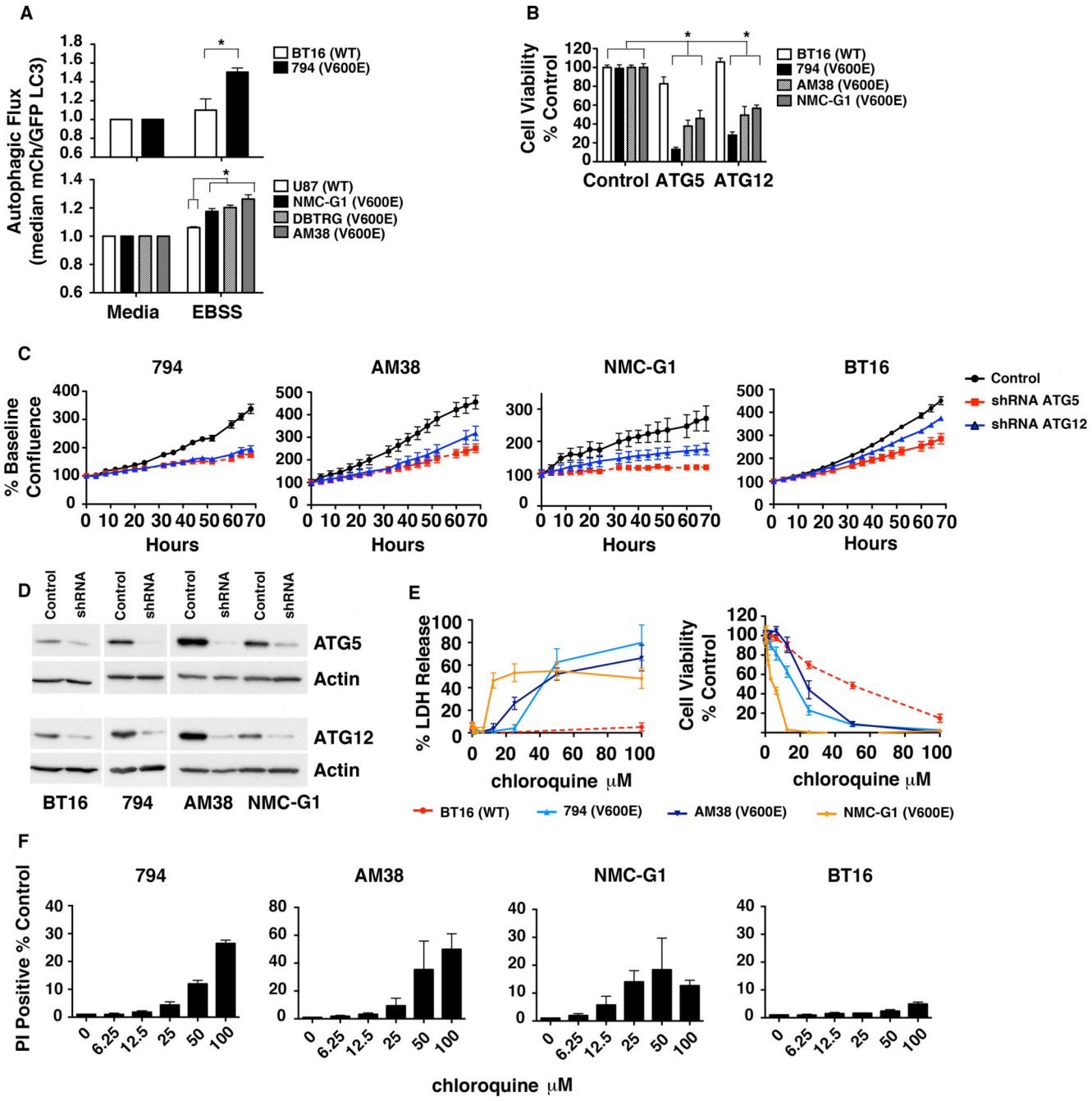

Figure 1.

CNS tumor cells with BRAF^{V600E} have high rates of induced autophagy and sensitivity to autophagy inhibition. (A) Cells with mCh-GFP-LC3 were exposed to either standard media or starvation EBSS media for 4 hours and analyzed for the change in ratio of mCh to GFP signal as a measure of autophagic flux. * $P < 0.05$. (B) Cells expressing control, ATG5, or ATG12 shRNAs were plated in standard media and allowed to grow for 72 hours before analysis by MTS assay. * $P < 0.05$. (C) Cells were plated as in (B) and were monitored every 4 hours by light microscopy using real time *in vitro* imaging. Quantitative analysis of confluence was performed using the IncuCyte system. Data shown are mean ± SEM of a

representative experiment. (D) Representative immunoblot demonstrating knockdown of baseline Atg5 and Atg12 protein levels after 72 hours of RNAi for experiments shown in (B–C). (E) WT BT16 and BRAF^{V600E} 794, AM38 and NMC-G1 mutant cells were treated with increasing doses of CQ for 48 hours and cell viability was evaluated by LDH release and MTS assay. (F) Cells were treated as in (E) and evaluated for the percentage of PI positive cells at 48 hours.

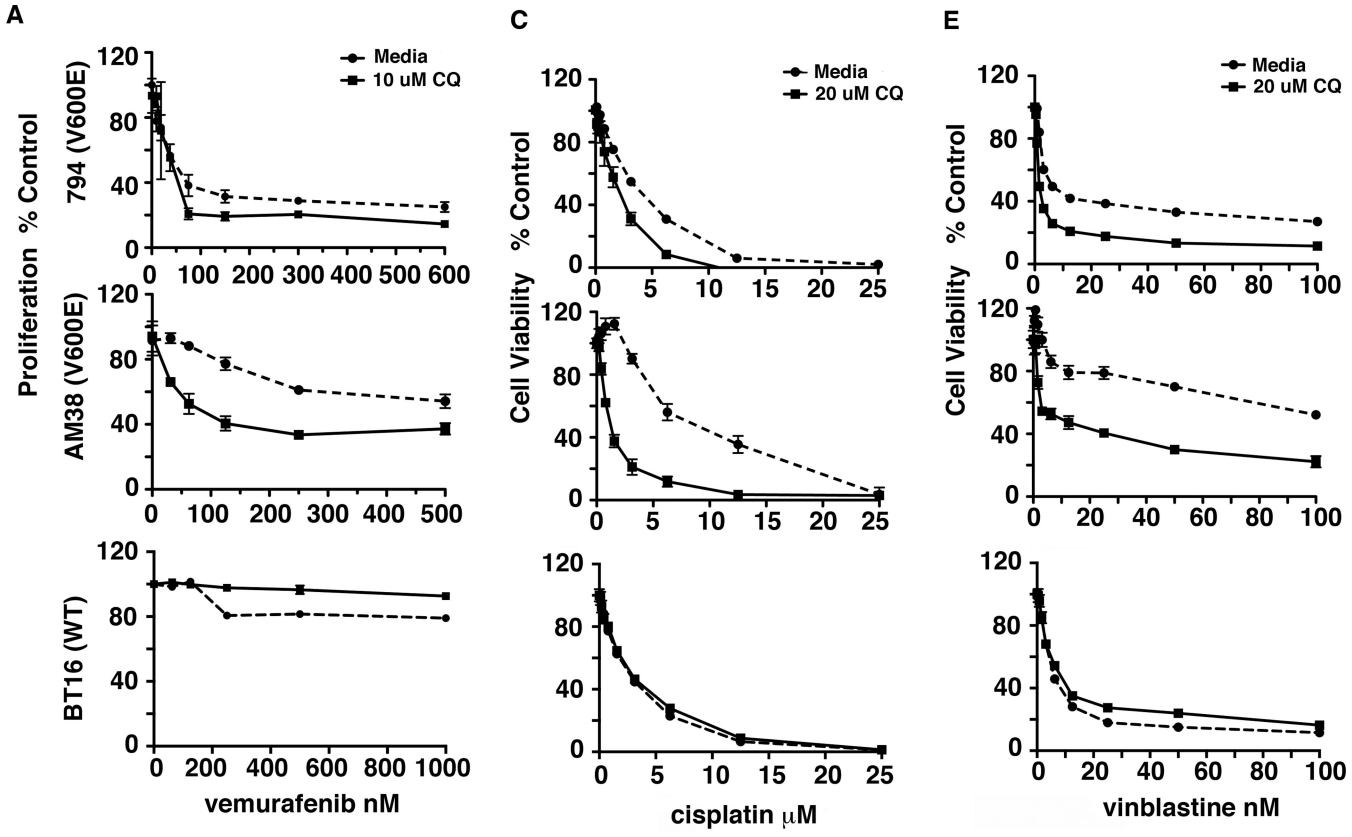

B

794

[CQ] μM	[vemurafenib] nM 9.375	18.75	37.5	75	150
2.5	0.80	0.97	0.93	0.61	0.56
5	0.89	0.83	0.91	0.82	0.61
10	0.90	0.92	0.68	0.67	0.37
20	0.57	0.50	0.89	0.83	0.14

AM38

[CQ] μM	[vemurafenib] nM 31.25	62.5	125	250	500
2.5	0.45	0.48	0.37	0.41	0.40
5	0.80	0.76	0.47	0.46	0.41
10	0.75	0.09	0.07	0.09	0.20
20	0.01	0.01	0.01	0.02	0.04

BT16

[CQ] μM	[vemurafenib] nM 62.5	125	250	500	1000
5	1.20	0.98	0.89	1.15	1.73
10	1.17	1.11	1.11	1.29	1.55
20	1.43	1.36	1.16	1.21	1.61
40	1.36	1.26	1.25	1.39	1.48

D

794

[CQ] μM	[cisplatin] μM 1.56	3.125	6.25	12.5
2.5	0.99	0.95	1.02	1.14
5	0.98	0.88	0.84	0.86
10	1.00	0.94	0.87	0.72
20	0.75	0.68	0.62	0.43
40	0.34	0.33	0.23	0.17

AM38

[CQ] μM	[cisplatin] μM 1.56	3.125	6.25	12.5
2.5	1.58	0.90	0.54	0.38
5	1.10	0.91	0.52	0.36
10	1.16	0.72	0.53	0.43
20	0.70	0.70	0.62	0.57
40	1.02	1.14	1.05	1.14

BT16

[CQ] μM	[cisplatin] μM 1.56	3.125	6.25	12.5
5	1.01	1.16	1.16	0.76
10	0.97	1.33	1.32	0.78
20	1.16	1.25	1.10	0.73
40	1.18	1.15	0.76	0.55

F

794

[CQ] μM	[vinblastine] nM 0.78	1.56	3.125	6.25
2.5	1.46	0.77	0.80	1.12
5	1.68	0.87	0.80	0.95
10	1.53	0.65	0.63	0.76
20	1.08	0.83	0.82	0.79
40	0.82	0.59	0.57	0.63

AM38

[CQ] μM	[vinblastine] nM 2.5	5	10	20
2.5	2.49	0.90	0.86	1.07
5	3.00	0.74	0.78	1.02
10	4.32	0.78	0.77	0.94
20	1.91	0.55	0.57	0.76
40	0.23	0.23	0.30	0.38

BT16

[CQ] μM	[vinblastine] nM 2.5	5	10	20
5	1.70	1.12	1.15	1.15
10	1.55	1.20	1.14	1.16
20	1.53	1.22	1.16	1.16
40	1.38	1.13	1.03	0.84

Figure 2.

Chloroquine improves tumor cell kill when used in combination with vemurafenib and chemotherapy in $BRAF^{V600E}$ mutant cells. (A) 794, AM38, and BT16 cells were treated with increasing doses of vemurafenib in media with and without 10 μM CQ for 72 hours and tritiated thymidine uptake assays were performed to assess cell proliferation. (B) 794, AM38, and BT16 cells were treated with increasing doses of vemurafenib and CQ for 72 hours. Tritiated thymidine uptake assays were performed to assess cell proliferation. The Chou-Talalay equation was used to calculate combination index (CI) values. CI values less

than 1, equal to 1 and more than 1 indicate synergism, additive effect, and antagonism, respectively. (C and E) 794, AM38, and BT16 cells were treated with increasing doses of cisplatin or vinblastine in media with and without 20 μM CQ for 72 hours and cell viability was evaluated by MTS assay. (D and F) 794, AM38, and BT16 cells were treated with increasing doses of cisplatin or vinblastine and CQ for 72 hours. MTS assays were performed to assess cell viability and CI values were calculated.

A

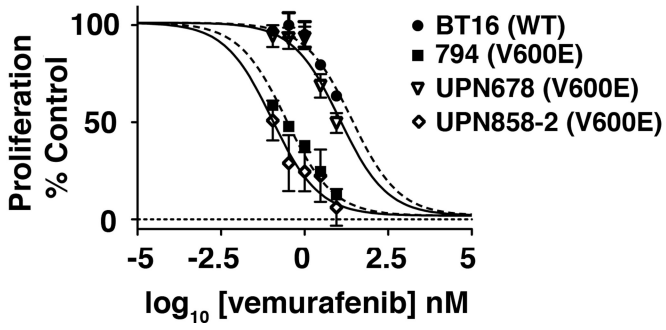

B

UPN678 (V600E)

[CQ] μM	[vemurafenib] μM 0.1	0.3	1	3	9
2.5	1.11	1.22	5.63	0.96	0.09
5	0.86	0.88	1.05	0.55	0.03
10	0.85	1.06	0.79	0.89	0.24

Figure 3.

(A) Short-term primary patient cultures of PXA tumor cells with $BRAF^{V600E}$ mutations, UPN858-2 and UPN678, and WT BT16 and $BRAF^{V600E}$ positive 794 cells were treated with increasing doses of vemurafenib for 72 hours and tritiated thymidine uptake assays were performed to assess cell proliferation. (B) UPN678 cells were treated with increasing doses of vemurafenib and CQ for 72 hours. Tritiated thymidine uptake assays were performed to assess cell proliferation and CI values were calculated as above.

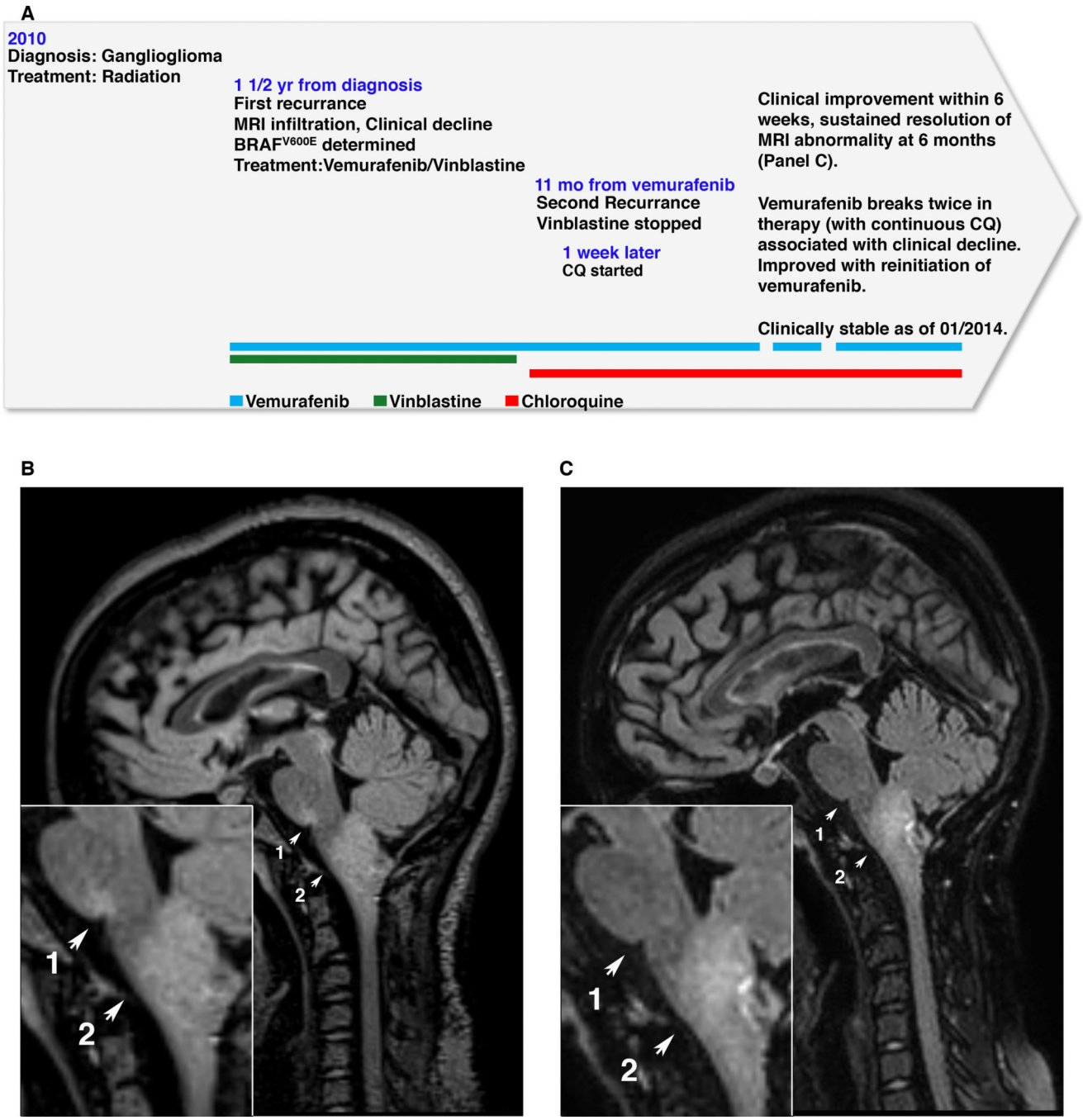

Figure 4.

Combination therapy with vemurafenib and autophagy inhibition improved MRI appearance of $BRAF^{V600E}$ brainstem ganglioglioma. (A) Clinical timeline schematic. (B) Sagittal FLAIR MR image acquired at the time of relapse of clinical symptoms demonstrates increased signal at the pontomedullary junction (arrow 1) that had previously resolved with treatment. (C) MR imaging following 6 months of combination vemurafenib plus CQ

therapy shows resolution of pontomedullary signal abnormality (arrow 1) and no further increase in size of the medullary tumor (arrow 2).